Structural inhomogeneity and piezoelectric enhancement in ZnO nanobelts

**Kasra Momeni · Anjana Asthana · Abhishek Prasad ·
Yoke K. Yap · Reza Shahbazian-Yassar**

Abstract In this work, piezoelectricity of individual ZnO nanobelts grown along the [0 1 $\bar{1}$ 0] direction is studied using piezoresponse force microscopy (PFM). It is found that the effective piezoelectric coefficient of these NBs, d_{33}^{eff}, is increasing from 2.7 pm/V at 30 kHz to 44 pm/V at 150 kHz. The results were explained by the Debye model, where structural inhomogeneity in our NBs was shown to be responsible for piezoelectric enhancement.

1 Introduction

Wurtzite zinc oxide (ZnO) is structurally noncentral symmetric, and thus applicable for piezoelectric devices. As ZnO has the highest piezoelectric tensor among tetrahedrally-bonded semiconductors [1], it becomes a promising candidate for sensor [2], actuator [3], and energy harvesting [4] applications. In particular, piezoelectricity of ZnO nanostructures has gained significant attention for nanoscale piezoelectronic devices. Several techniques including interferometry [5], scanning tunneling microscopy [6], and scanning probe microscopy (SPM) [7–9], have been used for measuring the piezoelectricity of materials. Piezoresponse

K. Momeni · R. Shahbazian-Yassar (✉)
Department of Mechanical Engineering, Michigan Technological University, Houghton, MI 49931, USA
e-mail: reza@mtu.edu

A. Asthana
Department of Materials Science and Engineering, Michigan Technological University, Houghton, MI 49931, USA

A. Prasad · Y.K. Yap
Department of Physics, Michigan Technological University, Houghton, MI 49931, USA

force microscopy (PFM), which is a modified atomic force microscopy (AFM) technique has been introduced recently for studying piezoelectric and ferroelectric properties of nanomaterials [10, 11]. A schematic figure of PFM setup used in our experiments is shown in Fig. 1. In this technique, an alternative voltage source is connected between the conductive AFM tip and bottom of the sample. The alternating voltage generates an alternating electric field inside the piezoelectric sample. The sample responds to the electric field by mechanical deformation due to inverse piezoelectric effect while AFM tip remains in contact with top of the sample. Out of plane deformation of the AFM tip will be measured by monitoring deflection of the AFM cantilever.

In fact, a few studies have been performed on piezoelectric properties of ZnO nanorods and nanobelts (NBs) but the results are controversial. Scrymgeour et al. [12] showed that the average value of the d_{33} piezoelectric coefficient of solution-grown ZnO nanorods to be around 4.41 pm/V. Moreover, the measured coefficient was independent of the frequency of the applied electric field in the range of 1–50 kHz. In contrast, Zhao et al. [13] have reported that the piezoelectric coefficient of ZnO NBs grown along the [2 $\bar{1}$ $\bar{1}$ 0] direction at 1400 °C was 26.7 pm/V at 30 kHz. This value reduced as a logarithmic function of frequency to 14.3 pm/V at 150 kHz. Interestingly, in the above studies, the role of defects on the electromechanical response was not studied systematically.

Electromechanical response of piezoelectric materials depends on their structure and configuration of defects [11, 14]. Configuration of such defects is in turn affected by synthesis parameters such as substrate material and annealing temperature [15]. Here, piezoelectricity of ZnO NBs grown along the [01 $\bar{1}$ 0] direction with (0001) top and bottom surfaces is reported. This is different from those reported with ZnO NBs grown along the [2 $\bar{1}$ $\bar{1}$ 0] direction [13].

Fig. 1 Schematic diagram of a piezoresponse force microscopy is shown. There is an alternative voltage source ($V_{ac} \cos \omega t$) between the conductive AFM tip and conductive substrate. Deflection of the cantilever will be monitored by position sensitive photo detector (PSPD). The feedback control on z-height gives the topography image while the lock-in amplifier provides piezo-response image
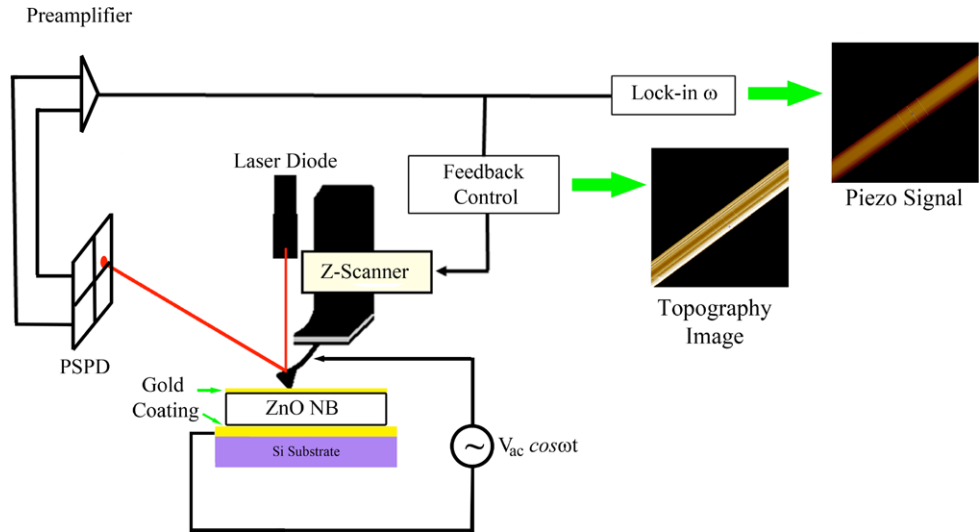
We found that the effective piezoelectric coefficients of $[0\,1\,\bar{1}\,0]$ ZnO NBs, d_{33}^{eff}, increased from 2.7 pm/V at 30 kHz to 44 pm/V at 150 kHz. Enhancement of d_{33}^{eff} was explained in terms of the Debye model, where coupling of elastic and dielectric effects are responsible for strengthening of piezo-electric.

2 Experimental procedure

Our ZnO NBs are grown by thermal Chemical Vapor Deposition (CVD) system as reported previously but without the use of gold catalyst [16]. These NBs are grown along the $[0\,1\,\bar{1}\,0]$ direction as confirmed by transmission electron microscopy (TEM) [17]. The two major facets of these NBs are (0001) and ($2\bar{1}\bar{1}0$). As-grown ZnO NBs were suspended in ethanol and a drop of the suspension was put on a Si substrate which was coated with a gold film (30 nm). Then, the whole sample surface was coated with another 2 nm thick gold film. The top gold layer acts as an electrode which provides uniform electric field inside the sample. This method is based on the integral method of excitation [18], which monitors the overall piezoelectric response of the sample rather than its local response. Figure 2 shows the clear contrast of a ZnO NB as measured by electric force microscopy (EFM). This confirmed that the top and bottom gold films are not short circuited.

The PFM measurements were conducted with a Si cantilever coated with a conductive layer of Platinum-Iridium. Stiffness of the cantilever was 40 N/m, and radius of curvature of the tip was 10 nm. A contact force was chosen to make sure that the measurements were in the strong-indentation regime [19]. This is the regime where piezoelectric response is dominated by the d_{33} value of the sample. PFM measurements were calibrated by calibration of the
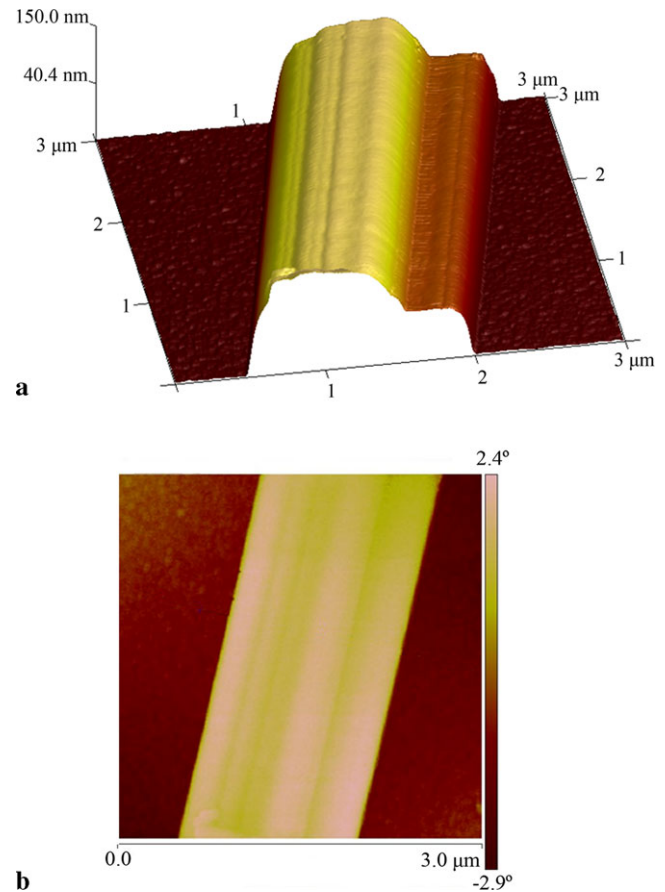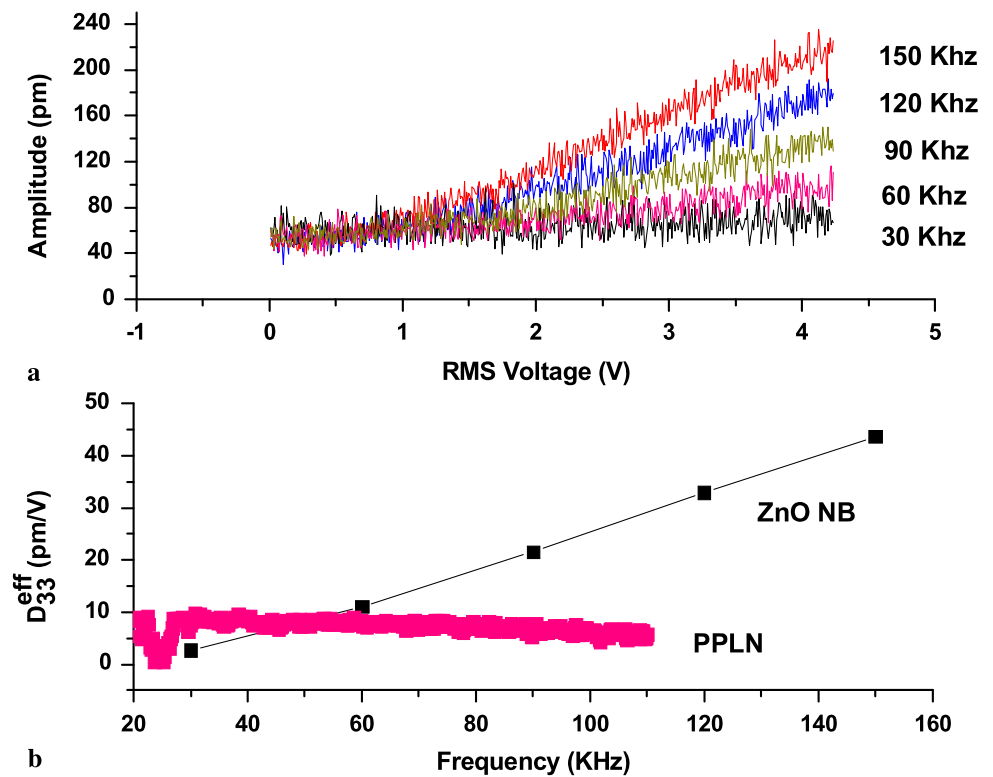
Fig. 2 (**a**) Topography and (**b**) EFM images of a ZnO nanobelt are shown. The sharp contrast between the NBs and substrate in the EFM image indicates that the NBs are not short circuited

photodiode response through force-distance curves on a sapphire sample [20]. Frequency dependence and background noise were removed following a background correction procedure described in the literature [21].

3 Results and discussion

Piezoelectric response of Periodically Poled Lithium Niobate (PPLN) was studied as our standard sample. The piezoelectric response of PPLN as a function of applied frequency is shown in Fig. 3b (red curve). It is shown that the piezoelectric response of PPLN ($\sim$8.2 pm/V) is independent of applied frequency and is in good agreement with the theoretical value of 8.07 pm/V reported in the literature [22].

The piezoresponse of the NB was measured by applying an alternating voltage between the tip and the substrate. Frequency of the applied electric field varied between 30 kHz and 150 kHz, which was far less than the resonance frequency of the cantilever. Deflection of the cantilever as a function of applied voltage (root mean square, RMS, value varied from 0–4 V) is shown in Fig. 3a. The slope of the deflection amplitude (A_f) versus applied RMS electric voltage (V_{rms}) gives the effective out-of-plane piezoelectric coefficient of material, d_{33}^{eff} [9], where $A_f = d_{33}^{\text{eff}} V_{rms}$. As shown in Fig. 3b (black curve), d_{33}^{eff} increases with the frequency of applied voltage (the so-called relaxation response) [23].

Elastic boundary conditions can significantly affect the measured d_{33}^{eff} values. If the NB has no constraint to lateral movement, $d_{33}^{\text{eff}} \approx d_{33}$ [24], where d_{33} is the actual piezoelectric coefficient. When the NB movement is laterally constrained, $d_{33}^{\text{eff}} = d_{33} - \frac{2S_{13}}{S_{11}+S_{12}} d_{31}$, where d_{ij} and S_{ij} are components of piezoelectricity and compliance tensors of the material, respectively. Substituting $d_{31} = -5.1$ pm/V [25]

and $d_{33} = 9.93$ pm/V [13], d_{33}^{eff} for the bulk ZnO was calculated to be $\sim$4.1 pm/V. The measured d_{33}^{eff} for ZnO NB at low frequencies ($\sim$30–40 kHz) was $\sim$2.7–5 pm/V, which is comparable to that of bulk ZnO [13]. It is interesting to note that substantially higher piezoelectric coefficients were obtained at high frequencies. The measured d_{33}^{eff} at 150 kHz was 44 pm/V (Fig. 3b, black curve), which was almost ten times greater than d_{33}^{eff} of bulk material.

The results show that piezoelectric coefficient of ZnO NBs is strongly frequency dependent, which is in agreement with Zhao et al. [13] data, but different in the following aspects: (1) In the same frequency range, the maximum d_{33}^{eff} obtained here is three-time greater than the maximum value obtained by Zhao et al. [13]. (2) Our d_{33}^{eff} values increase with the increase of applied frequency (relaxation behavior). However, Zhao et al. [13] observed a decrease in piezoelectric response by the increase of applied frequency. Similar relaxation behavior observed here has also been reported for single-phase anisotropic ferroelectrics and ferroelectric heterostructures [23] and piezoelectric materials with defects that are both elastic and electric dipoles [26]. The governing mechanism is referred as the Debye-type relaxation effect. This mechanism is based on heterogeneity of the material and coupling between the piezoelectric and dielectric properties. On the other hand, the retardation behavior [23] has been assumed to be related to the pinning of defects [13].

In the Debye model, a sample is considered to have defects that are both elastic and electric dipoles [26]. The po-
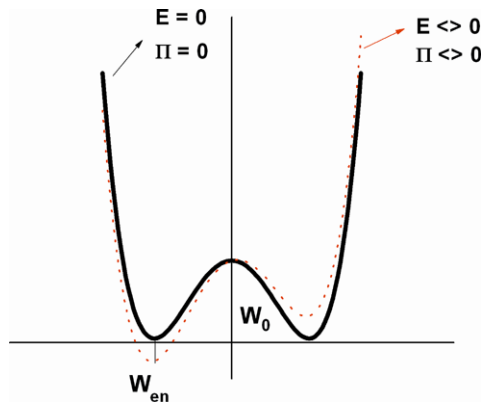
Fig. 4 Bistable potential function with (*black curve*) and without (*red curve*) external elastic, P, and electric, E, fields. W_0 is the height of the barrier and W_{en} is the energy change due to applying elastic and electric fields

tential energy function can be expressed in terms of bistable model as shown in Fig. 4. The difference in the electric energy of a dipole and elastic energy of a dipole is responsible for piezoelectric enhancement of the material which is formulated as follows.

Considering the polarization per volume due to defect (P) and strain per volume due to defect (x) is defined as follows:

$$P = n\mu \qquad (1a)$$

$$x = n\lambda \qquad (1b)$$

where μ, λ, and n show electric dipole, elastic dipole, and number of equally oriented dipoles per volume, respectively.

The constitutive equations of a piezoelectric material are [26]:

$$\vec{x} = \overset{\leftrightarrow}{\mathbf{S}}\vec{\Pi} + \overset{\leftrightarrow}{\mathbf{d}}\vec{E} \qquad (2a)$$

$$\vec{D} = \overset{\leftrightarrow}{\mathbf{d}}\vec{\Pi} + \overset{\leftrightarrow}{\varepsilon}\vec{E} \qquad (2b)$$

where x is the strain vector in Voigt notation, **S** is the elastic compliance tensor, $\vec{\Pi}$ is the stress vector in Voigt notation, **d** is the piezoelectric coefficient, $\vec{E}$ is the electric field vector, and ε is the dielectric permittivity tensor.

In presence of an alternating electric field $E = E_0 e^{i\omega t}$, and $P = P_0 e^{i\omega t}$ where E_0 and P_0 are the oscillation amplitude of piezoelectric fields, respectively, t is time, i is the imaginary number, and ω is the frequency of oscillation of the alternating electric source, the dielectric (**D**) and strain (**x**) tensors are:

$$D = \left[\varepsilon^\infty + \frac{n\mu^2}{kT(1+i\omega\tau)}\right]E + \left[d^\infty + \frac{n\mu\lambda}{kT(1+i\omega\tau)}\right]\Pi$$
$$(3a)$$

$$x = \left[d^\infty + \frac{n\mu\lambda}{kT(1+i\omega\tau)}\right]E + \left[S^\infty + \frac{n\lambda^2}{kT(1+i\omega\tau)}\right]\Pi$$

$$(3b)$$

where k is the Boltzmann constant, T is the temperature, and parameters with ∞ superscript indicate the value of those parameters at a very high frequency. Defining the piezoelectric coefficient d as

$$d = d^\infty + \frac{\Delta d}{1+i\omega\tau} \qquad (4)$$

where $\Delta d = n\mu\lambda/kT$. After separation of the real and imaginary components and defining $\Delta d = d^0 - d^\infty$, the piezoelectric coefficient can be defined as follows:

$$d = d^\infty + \frac{d^0 - d^\infty}{1+\omega^2\tau^2} - i\frac{(d^0 - d^\infty)\omega\tau}{1+\omega^2\tau^2} = d'(\omega) - id''(\omega)$$

$$(5)$$

Equation (5) has the same form as the well-known Debye equation [27]. It shows that the total piezoelectric coefficient has two parts, real part and imaginary part. Both real (d') and imaginary (d'') terms of piezoelectric constants are functions of frequency, ω. Real part of piezoelectric coefficient shows the effective piezoelectric constant, and the sign of $d^0 - d^\infty$ determines whether the material shows relaxation or retardation behavior. The sign of imaginary part of piezoelectric constant determines the rotation direction of the hysteresis curve, positive sign results in clockwise hysteresis while negative sign results in counter clock-wise hysteresis.

In order to verify that our ZnO NBs can be considered under the context of the Debye model, phase imaging using PFM was used to reveal the presence of domains in the ZnO NBs. The sample preparation steps for phase imaging were the same as discussed above, except in this case there was no top gold film on the sample surface so that local piezoresponse can be revealed. The cantilever spring constant and the applied AC bias were 40 N/m and 500 mV, respectively. Phase image of the ZnO NB shows different domains along the axis of the NB (Fig. 5a). These domains can be distinguished as bright contrast (positive phase angles: piezoresponse is phase lead the applied AC phase) and dark contrast (negative phase angles: piezoresponse is phase lag the applied AC phase). The distribution of phase oscillation was then characterized along the scanning path (white line) labeled on Fig. 5a. This scanning path mapped across the axis of the NB in Fig. 5b. Blue dotted lines show minimum and maximum values of phase along the scanning path which are corresponding to the blue crosses in Fig. 5a. As shown, the overall phases of these domains are negative (below zero degree) and suggesting for the Debye relaxation behavior. These domains can be formed due to formation of defects and change in the polarization of material for energy minimization or due to localized variations in synthesis
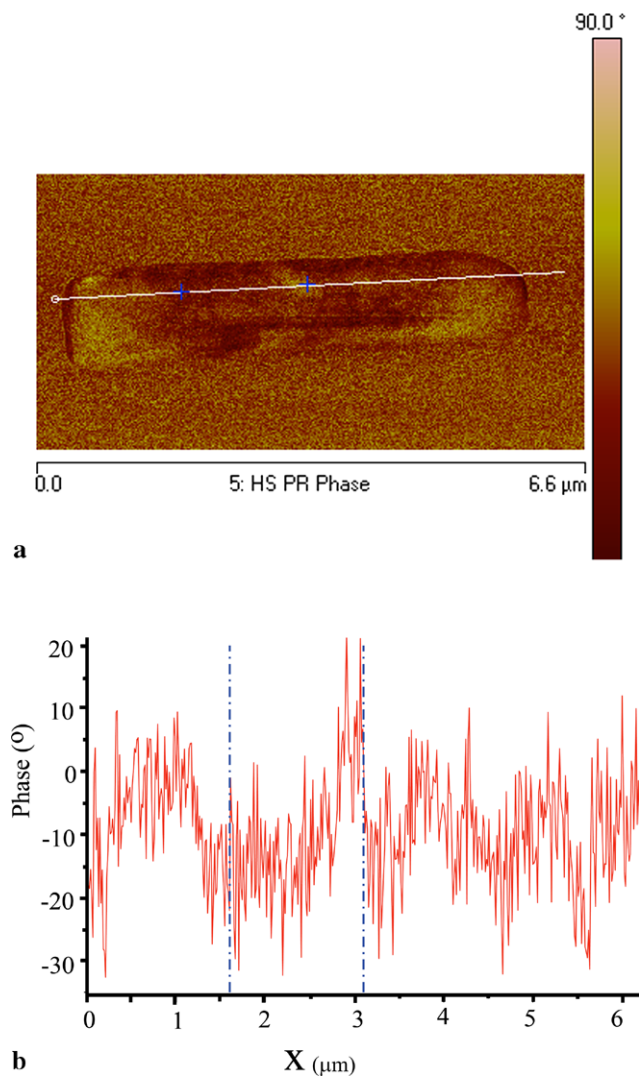
Fig. 5 (**a**) Phase image of piezoresponse of the ZnO NB shows domains along the axis of NB, (**b**) change in the phase of oscillation along the *white line* that is shown in (**a**). *Blue doted lines* represent the position of *blue crosses* in (**a**)
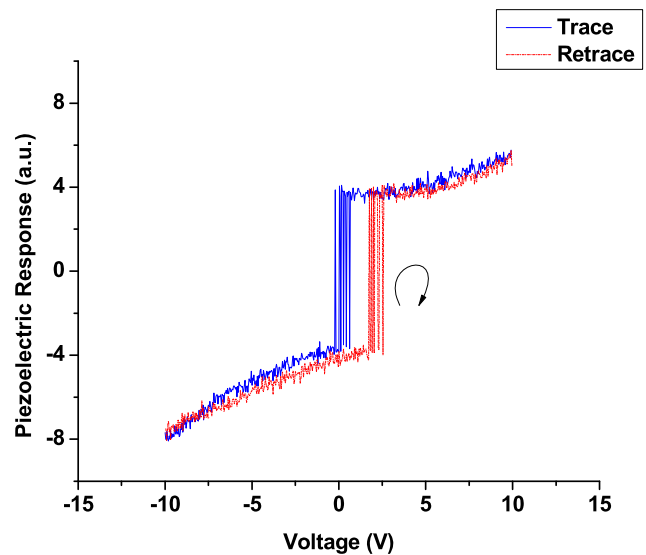

Fig. 7 Hysteresis curve of the as grown ZnO NB is shown. The *upper curve* shows the piezoelectric response of the material when the voltage increases from −10 V to 10 V (trace), and the *bottom curve* is the piezoelectric response of the material when the voltage reduces from 10 V to −10 V (retrace). The hysteresis curve has a clock-wise rotation direction which is in agreement with the proposed model, in case of relaxation behavior

conditions during the growth of NBs. Different types of defects may present in the structure of ZnO NBs such as twin boundaries (Fig. 6a, b), planar defects (Fig. 6c), and vacancies.

Considering materials with relaxation behavior, $\Delta d = d(0) - d(\infty) < 0$, the piezoelectric phase angle $\tan \delta_p = d''(\omega)/d'(\omega)$ is positive, which means the piezoelectric response proceeds the excitation. In the case of relaxation piezoelectric response, the hysteresis curve has a clockwise rotation angle. The hysteresis response of as grown ZnO NBs was measured by applying a DC voltage which varies from −10 to 10 V (Fig. 7).

The hysteresis curve in Fig. 7 shows a clockwise piezoelectric response. The blue curve shows the piezoelectric re-
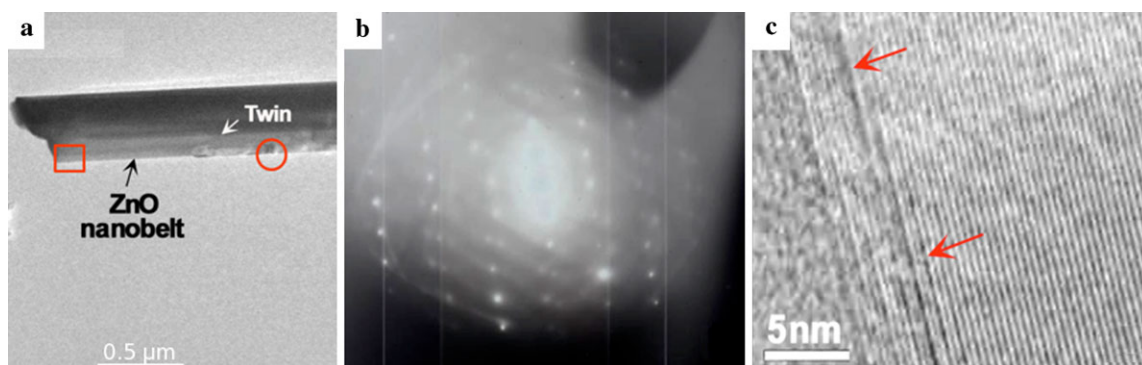

Fig. 6 (**a**) Low resolution image of twin boundaries, (**b**) diffraction pattern taken from a twin boundary region, and (**c**) high resolution TEM image of planar defects in ZnO NBs which shows structural inhomogeneity of the material

sponse of ZnO NBs when the applied electric voltage increased from −10 to 10 V. The red curve shows the piezoelectric response of ZnO NBs when the voltage has reduced from 10 to −10 V. Clockwise hysteresis curve indicates that the piezoelectric response (the imaginary part of piezoelectric coefficient) is ahead of excitation (the real part of piezoelectric coefficient), which is in agreement with the proposed model for piezoelectric materials with relaxation behavior.

Understanding the mechanism governing the frequency dependence of ZnO NBs would be a major step toward designing new sensors, actuators, and energy harvesting devices. Using the governing mechanism, new processing methods can be introduced for tailoring the piezoelectric properties of ZnO nanobelts and nanostructures. The results shown here suggest that the use of ZnO NBs with a better control on the defects density and structure may enable more efficient design of energy harvesting devices for high frequency sources, such as ultrasonic waves and turbulent flow.

4 Conclusion

In summary, we found that the piezoelectric properties of ZnO NBs can have relaxation behavior as a function of applied frequency. For low frequency measurements, the piezoelectric coefficient of our NBs was comparable to that of bulk ZnO. The coefficient was significantly increased by increasing frequency of the applied electric field, up to 44 pm/V at 150 kHz, sixteen times larger than that measured at 30 kHz. This is explained by the Debye model, where structural defects are responsible for formation of electric and elastic defects. The presence of domains was confirmed by PFM phase measurements. These results will form the basis for better understanding of piezoelectric properties of one-dimensional materials for their applications in nanoscale sensors, actuators, and generators.

References

1. A. Dal Corso, M. Posternak, R. Resta, A. Baldereschi, Phys. Rev. B, Condens. Matter Mater. Phys. **50**, 10715 (1994)
2. E. Comini, G. Faglia, G. Sberveglieri, Z. Pan, Z.L. Wang, Appl. Phys. Lett. **81**, 1869 (2002)
3. T. Shibata, K. Unno, E. Makino, Y. Ito, S. Shimada, Sens. Actuators A, Phys. **102**, 106 (2002)
4. Z.L. Wang, J. Song, Science **312**, 242 (2006)
5. A.L. Kholkin, C. Wutchrich, D.V. Taylor, N. Setter, Rev. Sci. Instrum. **67**, 1935 (1996)
6. R. Winters, M. Reinermann, C. Enss, G. Weiss, S. Hunklinger, Measurement of the piezoelectricity of films with scanning tunneling microscopy. Conf. Proc. **13**, 1316 (1995)
7. A.G. Agronin, Y. Rosenwaks, G.I. Rosenman, Nano Lett. **3**, 169 (2003)
8. J.A. Christman, J.R.R. Woolcott, A.I. Kingon, R.J. Nemanich, Appl. Phys. Lett. **73**, 3851 (1998)
9. C. Harnagea, A. Pignolet, M. Alexe, D. Hesse, U. Gösele, Appl. Phys. A, Mater. Sci. Process. **70**, 261 (2000)
10. V.V. Shvartsman, A.L. Kholkin, N.A. Pertsev, Appl. Phys. Lett. **81**, 3025 (2002)
11. A. Kholkin, I. Bdikin, D. Kiselev, V. Shvartsman, S.H. Kim, J. Electroceram. **19**, 83 (2007)
12. D.A. Scrymgeour, T.L. Sounart, N.C. Simmons, J.W.P. Hsu, J. Appl. Phys. **101**, 014316 (2007)
13. M.-H. Zhao, Z.-L. Wang, S.X. Mao, Nano Lett. **4**, 587 (2004)
14. A. Kholkin, Ferroelectrics **221**, 219 (1999)
15. L. Schuler, N. Valanoor, P. Miller, I. Guy, R. Reeves, M. Alkaisi, J. Electron. Mater. **36**, 507 (2007)
16. S.L. Mensah, V.K. Kayastha, Y.K. Yap, J. Phys. Chem. C **111**, 16092 (2007)
17. A. Asthana, K. Momeni, A. Prasad, Y.K. Yap, R.S. Yassar, Appl. Phys. Lett. **95**, 172106 (2009)
18. Review of Ferroelectric Domain Imaging by Piezoresponse Force Microscopy
19. S.V. Kalinin, D.A. Bonnell, Phys. Rev. B, Condens. Matter Mater. Phys. **65**, 125408 (2002)
20. M. Alexe, A. Gruverman, *Nanoscale Characterisation of Ferroelectric Materials: Scanning Probe Microscopy Approach* (Springer, Berlin, 2004)
21. T. Jungk, A. Hoffmann, E. Soergel, Appl. Phys. Lett. **89**, 163507 (2006)
22. M. Jazbinšek, M. Zgonik, Appl. Phys. B, Lasers Opt. **74**, 407 (2002)
23. D. Damjanovic, M.D. Maeder, P.D. Martin, C. Voisard, N. Setter, J. Appl. Phys. **90**, 5708 (2001)
24. J.-F. Li, P. Moses, D. Viehland, Rev. Sci. Instrum. **66**, 215 (1995)
25. F. Bernardini, V. Fiorentini, D. Vanderbilt, Phys. Rev. B, Condens. Matter Mater. Phys. **56**, R10024 (1997)
26. G. Bertotti, I.D. Mayergoyz, *The Science of Hysteresis* (Elsevier, Amsterdam, 2006)
27. P.J.W. Debye, *The Collected Papers of Peter J.W. Debye* (Interscience, New York, 1954)